Time-dependent stopping power and influence of an infinite magnetic field

Cord Seele,* Günter Zwicknagel,† Christian Toepffer, and Paul-Gerhard Reinhard
Institut für Theoretische Physik II, Universität Erlangen, D-91058 Erlangen, Germany
(Received 17 April 1997; revised manuscript received 29 July 1997)

Using the dielectric theory for a weakly coupled plasma we investigate the time-dependent behavior of the stopping power on a moving ion in a classical plasma. Special emphasis is placed on the transient properties between the onset of the external distortion (ion) and the stationary regime of constant stopping. It is shown that after a characteristic time of approximately a quarter of a plasma period τ_p the stopping power has reached its stationary value for a wide range of projectile velocities v_p, and coupling constants $\mathcal{Z}=Z_p/(4\pi n_0\lambda_D^3)$ (where Z_p is the charge number of the projectile, n_0 the electron density, and λ_D the Debye length). For small velocities v_p the stopping power then shows damped oscillations about the stationary value. Comparisons with the case of a one-dimensional dynamic associated with an infinite magnetic field show no significant further delay in this transient behavior. This result is confirmed by a phase mixing approximation: deviations from the stationary value occur with the same $t^{-3/2}$ law in either case. Furthermore, we present a Taylor series expansion for very short times where the pole expansion approach reaches its limits. Molecular-dynamics computer simulations have been done for the case without magnetic field. They are in good agreement with the theoretical results for weak coupling and reveal the importance of nonlinear effects for stronger coupled plasmas ($\mathcal{Z}\gg 1$). [S1063-651X(98)11602-1]

PACS number(s): 52.40.Mj, 61.85.+p

I. INTRODUCTION

Heavy ions lose energy when passing through a plasma. Recent applications are electron cooling of heavy ion beams and energy transfer for inertial confinement fusion [1,2]. Electron cooling is realized by mixing the ion beam periodically with a cooler electron beam of the same average velocity. The interaction length is normally about a few meters and the electron beam is guided by a magnetic field parallel to its direction of motion. The cooling of the ion beam may then be viewed as an energy loss in the common rest frame of both beams. Similar questions arise in heavy-ion-induced inertial confinement fusion. There a frozen hydrogen pellet is heated and compressed by stopping of (heavy) ion beams in the surrounding converter. In this case the electrons of the solid state converter are acting like a plasma and absorb the incoming energy.

So far, investigations have concentrated on the long-time behavior of the stopping power, both with and without magnetic field (e.g., [3]). Extensions to stronger coupled plasmas and nonlinear effects of ion stopping have been done by various methods of computer simulations: molecular-dynamics (MD) [4,5], particle-in-cell (PIC) [5,6], and Vlasov simulations [7,8]. Depending on the type of storage ring the interaction time between electron and ion beam is from some plasma periods τ_p down to $0.25\tau_p$ (ESR at GSI, Darmstadt). Therefore time-dependent considerations are quite important. We will focus on the time-dependent stopping power in the case of electron cooling but it is clear that any time-dependent effects are of great importance to inertial confinement fusion as well.

In Secs. II and III we will use the dielectric theory to study the time dependence of the energy loss. We will first apply it to the three-dimensional case with no external fields and later to a very strong magnetic field. Since any finite magnetic field leads to a very complex description already in the case of stationary stopping a feasible theoretical approach for a time-dependent description should at this stage consider the case of an infinite magnetic field where the electrons are constrained to a one-dimensional motion (while the much heavier ions are still allowed to move in all three dimensions). The only attempt known to us depends on an artificial cutoff parameter [9], which is not well motivated. Furthermore, this treatment presents results for the case of small and large ion velocities only whereas our approach is valid for all velocities. The full time dependence of the stopping power has to be evaluated numerically. For $t\ll\tau_p$ and $t\gg\tau_p$ we give in Secs. III C and IV some analytical approximations. Comparisons with MD simulations in Sec. V for the field-free case show a good agreement between both approaches for weak coupling but also reveal the importance of nonlinear effects for stronger coupling, which cannot be described by the dielectrical theory any more.

II. DIELECTRIC THEORY AND ASYMPTOTIC CONTRIBUTION

Within the dielectric theory the electron plasma is described as a continuous, polarizable fluid (medium), which is represented by the phase-space density of the electrons $f(\mathbf{r},\mathbf{v},t)$ alone as long as only a mean-field interaction between the electrons is considered and hard collisions are neglected. Such an approach is valid for weakly coupled plasmas where the number of electrons in the Debye sphere $N_D=4\pi n_0\lambda_D^3\gg 1$ [n_0 electron density, λ_D

*Present address: Max-Planck-Institut für Aeronomie, Max-Planck-Strasse 2, 37191 Katlenburg-Lindau, Germany.
†Present address: Laboratoire de Physique des Gaz et des Plasmas, Bâtiment 212, Université Paris XI, 91405 Orsay, France.

$=(\epsilon_0 k_B T/n_0 e^2)^{1/2}=$ Debye length] is very large. In this case the evolution of the distribution $f(\mathbf{r},\mathbf{v},t)$ is determined by the Vlasov-Poisson equation. The perturbation due to the projectile ion with charge Z_p enters as an external potential $\phi^{\rm ext}$, while the electrons feel the total potential $\phi(\mathbf{r},t)$, which is the sum of the external and a mean-field contribution, that is, an induced potential $\phi^{\rm ind}$. The induced potential causes the stopping power on the projectile ion defined as

$$\frac{dE}{ds}(\mathbf{v}_p,t)=-Z_p\hat{\mathbf{v}}_p\cdot\frac{\partial}{\partial\mathbf{r}}\phi^{\rm ind}(\mathbf{r},t)\bigg|_{\mathbf{r}=\mathbf{v}_p t}. \tag{1}$$

For a sufficiently small perturbation one can calculate the response of the target plasma and hence the stopping power by expanding the distribution function $f=f_0+f_1+f_2+\cdots$ and the total potential $\phi=\phi_1+\phi_2+\cdots$ in contributions of nth order in the external perturbation $\phi^{\rm ex}$. Even taking only the linear contributions is already a very demanding task when the translational invariance is lost in the boundary region of a plasma with finite extension. In many applications, however, the time the projectile spends in the boundary region is smaller than the transient time scale. In particular in an electron cooler, which is our main case of interest, the merging time of the ions and the electrons at the entrance of the cooler is much shorter than the transient time and the total time for passing the cooler section. Thus merging is essentially prompt. Furthermore, the ions have already penetrated some screening lengths into the electron target when the merging of the beams is finished. This allows one to consider the electron target as an infinitely extended, almost unperturbed system, where the perturbation due to the very fast previous interaction of the ions with the boundary layer should be negligible. For such kinds of conditions the problem of a transient regime in the stopping power can be attacked by assuming an unperturbed homogeneous target plasma with $f(t<0)=f_0$ and $\phi(t<0)=0$ and a sudden appearance of the ion with a velocity v_p at $t=0$ in the bulk of the electron plasma. In this model, keeping only terms that are linear in the external perturbation and after introducing scaled, dimensionless variables $r\to r/\lambda_D$, $v\to v/v_{\rm th}$, $t\to\omega_p t$, $\phi\to e\phi/(k_B T)$, $f\to v_{\rm th}^3 f/n_0$ with $v_{\rm th}^2=k_B T/m$ and $\omega_p=v_{\rm th}/\lambda_D$, we end up with the linearized Vlasov-Poisson equation in the form

$$\frac{\partial f_1}{\partial t}+\mathbf{v}\cdot\frac{\partial f_1}{\partial\mathbf{r}}+\frac{\partial\phi_1(\mathbf{r},t)}{\partial\mathbf{r}}\cdot\frac{\partial f_0}{\partial\mathbf{v}}=0, \tag{2}$$

$$\Delta\phi_1(\mathbf{r},t)=-4\pi\mathcal{Z}\delta(\mathbf{r}-\mathbf{v}_p t)\Theta(t)+\int d^3v f_1(\mathbf{r},\mathbf{v},t). \tag{3}$$

Here the first term on the right side of Eq. (3) reflects the external perturbation $\phi^{\rm ext}$ by the projectile with $\mathcal{Z}=Z_p/N_D$ and its sudden onset at $t=0$ described by the step function $\Theta(t)$. The second term defines the contribution from the induced potential

$$\Delta\phi^{\rm ind}=\int d^3v f_1(\mathbf{r},\mathbf{v},t). \tag{4}$$

Before proceeding further, we still have to comment on the validity of a linear description as given by Eqs. (2) and (3), that is, to quantify the strength of the perturbation caused by the ion. To this end we compare the potential energy $|Z_p|e^2/4\pi\epsilon_0 r$ for an electron at a distance r in the field of the ion with the kinetic energy $mv_r^2/2$ of the relative motion with velocity v_r. (For a heavy projectile the reduced mass can be replaced by the electron mass m.) Now we can assume a weak (local) perturbation whenever the potential energy is smaller than the kinetic one. Since we consider purely classical systems where no quantum effects will remove the singularity of the Coulomb potential, there always exists a critical distance r_c where the potential energy equals the kinetic energy and a strong perturbation occurs at distances $r<r_c$. The importance of this region of strong perturbation, however, depends on its size compared with the size of the whole interaction zone, which is approximatively bounded by $r<\lambda$, where λ represents the velocity dependent screening length. From this picture we can deduce a criterion for a globally weak perturbation by demanding a small ratio of the critical distance r_c to the screening length λ:

$$\frac{r_c}{\lambda}=\frac{2|Z_p|e^2}{4\pi\epsilon_0 m\langle v_r\rangle^2\lambda}=\frac{2|Z_p|}{N_D\langle v_r/v_{\rm th}\rangle^2(\lambda/\lambda_D)}\approx\frac{\mathcal{Z}}{1+v_p^3}\ll 1. \tag{5}$$

Here we used the definition of r_c for an averaged energy of relative motion indicated by the average $\langle\cdots\rangle$ over the velocity distribution of the electrons. The screening length λ is at low projectile velocities and for weakly coupled plasmas just the Debye length λ_D while it becomes for high projectile velocities $\lambda\approx v_p/\omega_p$ (unscaled) $=\lambda_D v_p$ (with v_p in units of $v_{\rm th}$). The averaged relative velocity can be approximated by the thermal velocity $v_{\rm th}$ for small projectile velocities and by the projectile velocity v_p for fast projectiles. A simple interpolation between the low and high velocity values of λ and $\langle v_r\rangle$ and the suppression of a factor 2 yields then the final expression $\mathcal{Z}/(1+v_p^3)$ in Eq. (5), which represents the desired linearization parameter. For a discussion of more general expressions for the strength of the perturbation that include quantum effects as well see [10]. Besides this simple physical picture we used to derive the linearization parameter one can alternatively inspect the scaled equations and their solutions. As already obvious from Eq. (3) the strength of the perturbation will be proportional to $\mathcal{Z}$. To work out also the velocity dependence of the linearization parameter requires, however, solving the set of equations of next higher, i.e., second, order in the perturbation. This has been done, for instance, in [2] and yields as well criterion (5).

As a first step towards the stopping power (1) the induced potential $\phi^{\rm ind}$ can be calculated from the linearized Vlasov-Poisson Equations (2) and (3) after applying a Fourier-Laplace transform $[(\mathbf{r},t)\to(\mathbf{k},s)]$. From

$$[\phi^{\rm ind}(\mathbf{k},s)+\phi^{\rm ext}(\mathbf{k},s)]\left[1+\frac{1}{k^2}\int d^3v\,\mathbf{k}\cdot\frac{\partial f_0}{\partial\mathbf{v}}\frac{1}{is-\mathbf{k}\cdot\mathbf{v}}\right]=\phi^{\rm ext}(\mathbf{k},s), \tag{6}$$

we obtain the dielectric function $\varepsilon(\mathbf{k},s)$ by the usual definition

$$\phi_1=\phi^{\mathrm{ind}}(\mathbf{k},s)+\phi^{\mathrm{ext}}(\mathbf{k},s)=\phi^{\mathrm{ext}}(\mathbf{k},s)/\varepsilon(\mathbf{k},s) \tag{7}$$

as

$$\varepsilon(\mathbf{k},s)=1+\frac{1}{k^2}\int d^3v\frac{\mathbf{k}\cdot\partial f_0/\partial\mathbf{v}}{is-\mathbf{k}\cdot\mathbf{v}}. \tag{8}$$

No assumption had yet to be made on f_0.

A. Absence of magnetic field

Assuming a three-dimensional Maxwellian distribution for $f_0=(2\pi)^{-3/2}\exp(-v^2/2)$, the dielectric function (8) turns into (cf. [11,12])

$$\begin{aligned}\varepsilon(k,s)&=1+\frac{1}{k^2}\frac{1}{\sqrt{2\pi}}\int dv_\parallel\frac{v_\parallel\exp(-v_\parallel^2/2)}{v_\parallel-is/k}\\&=1+\frac{1}{k^2}\{1+i\sqrt{\pi}\zeta\exp(-\zeta^2)[\mathrm{erf}(i\zeta)+1]\}\\&=1+\frac{1}{k^2}[X(\zeta)+iY(\zeta)],\end{aligned} \tag{9}$$

where $v_\parallel$ is the velocity component parallel to the wave vector $\mathbf{k}$, $\zeta=is/k\sqrt{2}$, and X,Y denote the real and imaginary parts of the dispersion function, respectively. The dielectric function ε (9) only depends on the magnitude of k and not on its direction any more, since we consider an isotropic plasma. It has the important property

$$\varepsilon(k,s)=\varepsilon^*(k,s^*). \tag{10}$$

In terms of the dielectric function and with help of relation (7), the stopping power as defined in Eq. (1) reads now in Fourier-Laplace space

$$\begin{aligned}\frac{dE}{ds}(\mathbf{v}_p,t)=&-\frac{4\pi\mathcal{Z}Z_p}{i(2\pi)^4}\int d^3k\frac{i\mathbf{k}\cdot\hat{\mathbf{v}}_p}{k^2}\\&\times\int_{-i\infty+\delta}^{i\infty+\delta}ds\,\frac{i}{is-\mathbf{k}\cdot\mathbf{v}_p}\left[\frac{1}{\varepsilon(k,s)}-1\right]\\&\times\exp(i\mathbf{k}\cdot\mathbf{v}_pt)\exp(st),\end{aligned} \tag{11}$$

with $\delta\to0^+$. We will refer to the scaled stopping power if the energy loss is divided by $\mathcal{Z}Z_p$. In consistency with Eq. (3) we get $dE/ds=0$ for $t<0$ by closing the contour of integration in the right half-plane of the complex s plane. For $t>0$ we can close the contour in the left half-plane yielding a sum over all enclosed poles s_j. Splitting off the contribution from the pole on the imaginary axis leads to

$$\frac{dE}{ds}(\mathbf{v}_p,t)=-\frac{\mathcal{Z}Z_p}{2\pi^2}[\mathcal{A}(\mathbf{v}_p)+\mathcal{D}(\mathbf{v}_p,t)], \tag{12}$$

where

$$\mathcal{A}(\mathbf{v}_p)=\int d^3k\frac{i\mathbf{k}\cdot\hat{\mathbf{v}}_p}{k^2}\left[\frac{1}{\varepsilon(k,-i\mathbf{k}\cdot\mathbf{v}_p)}-1\right], \tag{13}$$

$$\begin{aligned}\mathcal{D}(\mathbf{v}_p,t)=&\int d^3k\frac{i\mathbf{k}\cdot\hat{\mathbf{v}}_p}{k^2}\exp(i\mathbf{k}\cdot\mathbf{v}_pt)\\&\times\sum_j\mathrm{Res}\left[\frac{1}{\varepsilon(k,s)}\right]\frac{i\exp(st)}{is-\mathbf{k}\cdot\mathbf{v}_p}\bigg|_{s=s_j}.\end{aligned} \tag{14}$$

While Eq. (13) is independent of t and yields the asymptotic contribution to the stopping power, Eq. (14) depends on time and describes the exponentially decaying dynamic contribution. The time-independent asymptotic contribution (13) can be evaluated further. Due to the singularity of the Coulomb potential the k integral shows a divergence for large k. Guided by the binary collision model a cutoff $k_{\max}$ is introduced, which corresponds to the inverse of the impact parameter for hard scattering events with a deflection angle larger than 90° for the given mean relative velocity $\langle|\mathbf{v}_p-\mathbf{v}|\rangle$. In units of $1/\lambda_D$ and employing the scaling from above this cutoff reads [2]

$$k_{\max}=\frac{v_p^2+2}{|\mathcal{Z}|}. \tag{15}$$

In terms of the real and imaginary parts of the dispersion function (9) the asymptotic contribution in the field-free case is [2,13]

$$\mathcal{A}(v_p)=\frac{2\pi}{v_p^2}\int_0^{v_p/\sqrt{2}}d\xi\xi\left\{Y(\xi)\ln\frac{[k_{\max}^2+X(\xi)]^2+Y^2(\xi)}{X^2(\xi)+Y^2(\xi)}+2X(\xi)\left[\arctan\frac{X(\xi)}{Y(\xi)}-\arctan\frac{k_{\max}^2+X(\xi)}{Y(\xi)}\right]\right\}. \tag{16}$$

Here $\xi=\mu v_p/\sqrt{2}$ and μ denotes the cosine between $\mathbf{k}$ and $\mathbf{v}_p$. For the purely real argument ξ the real and imaginary parts of the dispersion function Eq. (9) take the form

$$X(\xi)=1-2\xi\exp(-\xi^2)\int_0^\xi\exp(t^2)dt,\quad Y(\xi)=\sqrt{\pi}\xi e^{-\xi^2}. \tag{17}$$

Using Eqs. (16) and (17) analytical expressions for the asymptotic contribution to the stopping power (12) can be obtained in the limits of small and large ion velocities and for linear (weak) coupling, i.e., $k_{\max} \gg 1$. This yields

$$\frac{dE}{ds} \approx -\frac{v_p}{3}\sqrt{\frac{2}{\pi}}\ln(k_{\max}), \quad v_p \ll 1,$$
$$\frac{dE}{ds} \sim -\frac{1}{v_p^2}\ln(k_{\max} v_p), \quad v_p \gg 1. \tag{18}$$

B. Infinite magnetic field

For the one-dimensional motion of the plasma electrons in an infinite magnetic field we have to take a slightly different initial electron distribution f_0 in Eq. (8): there is only a Maxwellian distribution in the direction of the magnetic field. The transversal motion perpendicular to the field lines is completely quenched and thus also the perturbation f_1 depends only on $v_\parallel$. We note that this case has to be distinguished from the case of a plasma with a temperature anisotropy $\lambda = T_\perp / T_\parallel$ (with respect to $\mathbf{v}_p$) where f_1 may depend on $v_\perp$ even in the case $\lambda \to 0$. In view of Eq. (9) we can now write

$$\varepsilon(k,k_\parallel,s) = 1 + \frac{1}{k^2}\frac{1}{\sqrt{2\pi}}\int dv_\parallel \frac{v_\parallel \exp(-v_\parallel^2/2)}{v_\parallel - is/k_\parallel} = 1 + \frac{1}{k^2}[X(\zeta_\parallel) + iY(\zeta_\parallel)]. \tag{19}$$

Due to the additional direction, which is significant, we have introduced $\zeta_\parallel = is/(|k_\parallel|\sqrt{2})$ with $k_\parallel$ being the component of $\mathbf{k}$ parallel to $\mathbf{B}$. Following the calculation of the previous section, we are only interested in the undamped mode ($s = -i\mathbf{k}\cdot\mathbf{v}_p$) for the asymptotic contribution. For simplicity we will only consider the special case of the ion moving parallel to the magnetic field: $\mathbf{v}_p \| \mathbf{B}$. Using the symmetry properties of the dielectric function, this contribution can be calculated exactly:

$$\mathcal{A}_\infty(v_p) = \frac{\pi}{2}\left[Y(\xi)\ln\frac{[k_{\max}^2 + X(\xi)]^2 + Y^2(\xi)}{X^2(\xi) + Y^2(\xi)} + 2X(\xi)\left(\arctan\frac{X(\xi)}{Y(\xi)} - \arctan\frac{k_{\max}^2 + X(\xi)}{Y(\xi)} \right) \right], \tag{20}$$

where $\xi = v_p/\sqrt{2}$ and $X(\xi), Y(\xi)$ as given in Eq. (17). In contrast to the three-dimensional case (16) the stopping power at infinite magnetic field (20) is for high velocities $v_p \gg 1$ [3]

$$A_\infty(v_p \gg 1) \sim (\pi/v_p)^2 \tag{21}$$

and thus independent of $k_{\max}$. The cutoff $k_{\max}$ necessary at low ion velocities $v_p \lesssim 1$ is, however, less well defined here than for the three-dimensional electron motion, where the cutoff (15) was deduced from the binary collision picture. Now, the electrons are forced to move parallel to **B**. Since we assumed the motion of the ion in this direction as well the ion and an electron just pass each other along a straight line. For symmetry reasons the total momentum transfer and the stopping power are zero. Purely binary interactions contribute nothing and the stopping of the ion is only due to the collective response of the plasma, that is, due to modes with long wavelengths $k \lesssim 1/\lambda_D$. This suggests taking $k_{\max}$ of the order of $1/\lambda_D$, but further investigations are clearly needed here for a more precise description of the asymptotic stopping power in this particular case. This problem, however, is of minor importance for the transient behavior of the stopping power and will not be considered further since the transient behavior is almost independent of $k_{\max}$. A change of the cutoff $k_{\max}$ of course changes the asymptotic value at low ion velocities, but the fully dynamic stopping power in units of the asymptotic one is affected only slightly.

III. DYNAMIC CONTRIBUTION

After this short overview on the asymptotic contributions to the stopping power we now turn towards the dynamics. As we have already stated in connection with Eqs. (12)–(14) the zeros of the dielectric function

$$\varepsilon(k, s_j(k)) = 0 \tag{22}$$

are responsible for the transient behavior. To get an impression on the structure and the zeros of $\varepsilon(k,s)$, Fig. 1 shows a contour plot of the inverse dielectric function in the complex s plane for $k = 0.5$. The symmetry (10) is clearly visible. The inverse of the dielectric function reveals an infinite number of poles located in the complex s plane at positions $s_j(k)$, which are ordered according to decreasing $\mathrm{Re}(s_j)$. The variation with k is addressed in Fig. 2 for the first two poles s_0, s_1. In contrast to all further poles that show a similar strong damping $\mathrm{Re}(s)/\mathrm{Im}(s) \approx 1$ as s_1 (short dashes), the plasmon pole s_0 (solid curves) has the outstanding features of vanishing damping and a nonzero frequency for small k. In the limit $k \to 0$, where we have $|\mathrm{Re}(s_0)/\mathrm{Im}(s_0)| \ll 1$ and $|\zeta| \gg 1$, the dielectric function Eq. (9) can be expanded to get the well-known analytical solution of $\varepsilon(k, s(k)) = 0$ [12]

$$s_0(k) \approx -i\sqrt{1+3k^2} - \sqrt{\frac{\pi}{8}}\frac{1}{k^3}\exp\left(-\frac{1+3k^2}{2k^2} \right), \tag{23}$$

which describes the dispersion of plasma waves. Here the second term, which vanishes exponentially for $k \to 0$, repre-

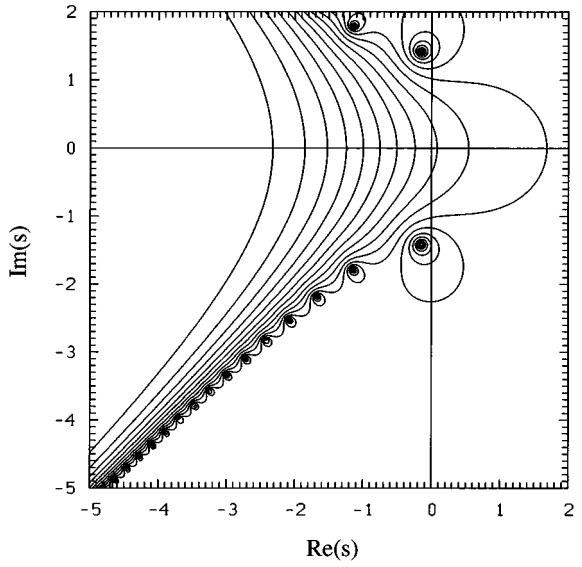

FIG. 1. Contour plot of the inverse dielectric function $|\varepsilon(k,s)|^{-1}$ in the complex s plane for $k=0.5$. Note the symmetry about $\mathrm{Im}(s)=0$. The pole closest to $\mathrm{Re}(s)=0$ corresponds to the plasmon pole $s=s_0(k)$.

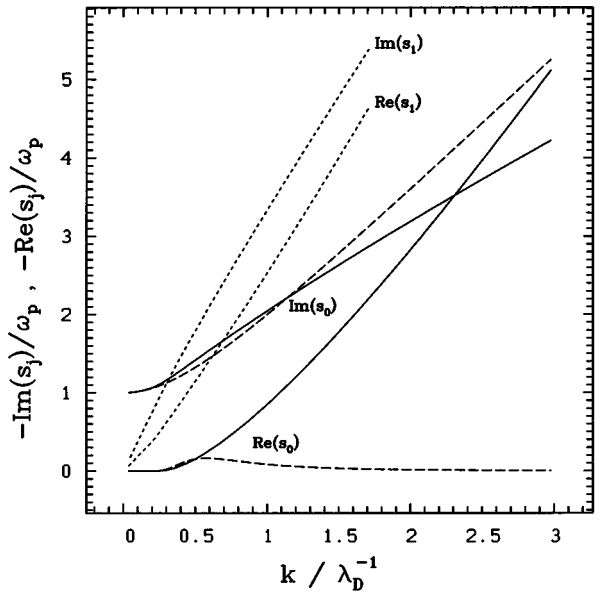

FIG. 2. Real and imaginary parts of numerically determined dispersion relations $s_j(k)$ in terms of the plasma frequency ω_p. The solid curve shows the plasmon pole $s_0(k)$, the short-dashed ones the pole $s_1(k)$. The analytically obtained expression for $s_0(k)$, Eq. (23), is given by the long dashes.

sents the Landau damping caused by the transfer of energy from the collective to the single-particle motion. The range of validity of solution (23) is shown as well in Fig. 2 by comparison with the full numerical result; see the long-dashed and solid curves, respectively.

While the weakly damped plasmon pole s_0 may be of importance for the long time behavior, the infinite number of strongly damped further modes s_j can well be neglected in this case. For the short time behavior of the stopping power, however, they play a key role. As we are interested exactly in this case, we have to determine the functions $s_j(k)$ needed for the dynamic contribution Eq. (14). Since no analytical treatment for solving the dispersion relation is available in general, this has been done by a numerical evaluation of Eq. (22) for a huge range of k and large number of poles s_j.

A. Absence of magnetic field

Before we can analyze the dynamic contribution (14) any further we will calculate the residue for the jth pole of the inverse dielectric function:

$$\mathrm{Res}\frac{1}{\varepsilon(k,s)}\bigg|_{s=s_j}=\frac{1}{\partial_s\varepsilon(k,s)}\bigg|_{s=s_j}=\frac{-s_jk^2}{s_j^2+k^2+1}. \tag{24}$$

Using the symmetry relation (10) for the dielectric function ensures the dynamic contribution to be real since for every pole s_j there is its complex conjugate s_j^*. Letting the j sum in Eq. (14) run over all complex pairs of poles and introducing polar coordinates ($\mu=\hat{\mathbf{k}}\cdot\mathbf{v}_p$) we find

$$\mathcal{D}(v_p,t)=\frac{4\pi}{v_p^2}\int_0^\infty dkk^3\int_{-v_p}^{v_p}d\mu\mu\sum_j\mathrm{Re}\left(\frac{s_je^{-i(is_j-k\mu)t}}{(s_j^2+k^2+1)(is_j-k\mu)}\right). \tag{25}$$

Knowing $\mathrm{Re}[s_j(k)]<0\ \forall k,j$ allows us to rewrite this with the aid of an integral representation

$$\int_{-v_p}^{v_p}d\mu\mu\frac{\exp[-i(is_j-k\mu)t]}{is_j-k\mu}=i\int_{-v_p}^{v_p}d\mu\mu\int_t^\infty d\tau\exp[-i(is_j-k\mu)\tau]=-2\int_t^\infty d\tau\left[\frac{\sin(kv_p\tau)}{(k\tau)^2}-\frac{v_p\cos(kv_p\tau)}{k\tau}\right]\exp(s_j\tau). \tag{26}$$

With $\alpha_j(k)=\mathrm{Re}[s_j(k)]$ and $\beta_j=\mathrm{Im}[s_j(k)]$, the real part in Eq. (25) can be evaluated further. We finally obtain for the dynamic contribution

$$\mathcal{D}(v_p,t)=-8\pi\int_0^{k_{\max}}dkk^3\int_t^\infty d\tau\left[\frac{\sin(kv_p\tau)}{(kv_p\tau)^2}-\frac{\cos(kv_p\tau)}{kv_p\tau}\right]\sum_j\frac{e^{\alpha_j\tau}}{N_j}[S_{1j}\alpha_j\cos(\beta_j\tau)+S_{2j}\beta_j\sin(\beta_j\tau)], \tag{27}$$

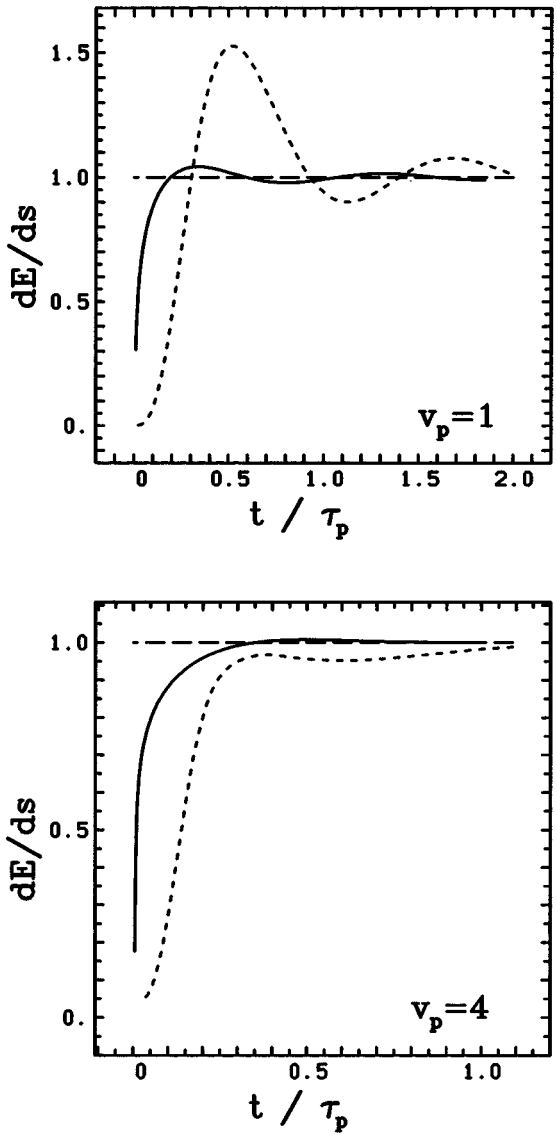

FIG. 3. Results of the full dielectric treatment of the stopping power in case of no (solid curve) and infinite (short-dashed curve) magnetic field B for $\mathcal{Z}=0.03$ and $v_p=1$ and 4. For better comparison the data are given in units of the appropriate asymptotic values (long-dashed line) of Table I.

where the sum runs over all pairs of complex poles of the dielectric function (cf. Fig. 1) and we have used the following abbreviations:

$$N_j=(\alpha_j^2-\beta_j^2+k^2+1)^2+4\alpha_j^2\beta_j^2,$$
$$S_{1j}=\alpha_j^2+\beta_j^2+k^2+1, \tag{28}$$
$$S_{2j}=\alpha_j^2+\beta_j^2-k^2-1.$$

It should be noted that the upper cutoff parameter $k_{\max}$ in Eq. (27) is kept only for reasons of consistency, since all dynamic contributions are exponentially damped for $t>0$. The expression (27) has to be calculated numerically. The results for various projectile velocities v_p and coupling strengths $\mathcal{Z}$ reveal that the stopping power is typically switched on during a quarter of the plasma period τ_p, as shown in Fig. 3 (solid curves). The damped oscillations about the mean rise to the asymptotic value are more pronounced for small velocities v_p, which yields the tendency towards a somewhat shorter transient regime at high v_p. The absolute values of the asymptotic contribution are given in Table I.

TABLE I. Asymptotic values of the scaled stopping power $-dE/ds$ (in units of k_BT_e/λ_D) for various ion velocities v_p.

	$B=0$			$B=\infty$[a]
	$\mathcal{Z}$			
$v_p/v_{\rm th}$	0.03	0.94	19.4	
1	0.8590	0.1831	[b]	0.0435
4	0.4788	0.2632	0.0747	0.0411
7	0.1909	0.1204	0.0588	0.0109
12	0.0762	0.0522	0.0312	0.0035

[a]$k_{\max}$ in Eq. (20) is set to $1/\lambda_D$; scaled stopping power is therefore independent of $\mathcal{Z}$.
[b]Breakdown of dielectric description.

The numerical integration gets more and more involved with decreasing t since more and more poles of the dielectric function have to be taken into account. Here we included up to 200 poles. For the short-time behavior other techniques must be used. For that purpose we study in Sec. IV A Taylor series expansion of the stopping power.

B. Infinite magnetic field

Since the dielectric function changes in the magnetized case (19) we have to expect a different solution of the dispersion relation (22) too. If we focus on the special case $\mathbf{v}_p\|\mathbf{B}$, as in Sec. II B, an analysis of the root condition reveals that we can still use our data of the pole functions $s_j(k)$ if we make the following substitution in Eq. (14):

$$s_j(k)\rightarrow|\mu|s_j(k), \tag{29}$$

with μ denoting the cosine of the angle between $\mathbf{k}$ and $\mathbf{k}_\|$. This can be interpreted as a frequency shift to lower values and reduced damping for waves propagating with a transversal component to the magnetic field. This anisotropy is not surprising since the electrons in these waves are bound to a one-dimensional motion parallel to $\mathbf{B}$. Following the same considerations as in Sec. III A we obtain a result similar to the field-free case, except for an additional integration reflecting the loss in symmetry

$$\mathcal{D}(v_p,t)=-8\pi\int_0^{k_{\max}}dkk^3\int_t^\infty d\tau\int_0^1 d\mu\mu^2\sin(\mu kv_p\tau)$$
$$\times\sum_j\frac{e^{\mu\alpha_j\tau}}{N_j}[S_{1j}\alpha_j\cos(\mu\beta_j\tau)+S_{2j}\beta_j\sin(\mu\beta_j\tau)]. \tag{30}$$

Here we have used the same abbreviations (28) as before.

A numerical solution of the dynamic contribution is shown in Fig. 3 [with $k_{\max}$ set to $1/\lambda_D$, see the remark below Eq. (20)]. It is scaled to the asymptotic contribution (20) in order to compare the time evolution with the field-free case.

There seems to be a slight delay of about $0.1\tau_p$ in the onset of the stopping power in case of an infinite magnetic field. In the case of a slow projectile velocity $v_p \leqslant 1$ there is even an excess in the transient period about $0.5\tau_p$.

C. One-pole approximation

In order to not rely on numerical results only, we give an admittedly crude approximation for determining the temporal behavior of the stopping power close to the stationary regime. It turns out to be in good agreement with the previous results. Let us consider a situation with no magnetic field first. Looking at Eq. (27) and taking into account the nature of the poles (cf. Figs. 1 and 2), we notice that upon approaching the stationary case only one pole remains dominant: the plasmon pole s_0. Considering only small velocities $v_p < 1$ the dominant contribution to Eq. (27) arises from the integration over small k, while for higher k the oscillating term rapidly goes to zero.

In the following approximation we neglect the Landau damping term and consider only phase mixing of the integrand for small k, where $\mathrm{Im}[s_0(k)] \approx -\sqrt{1+3k^2}$ (23). Applying a stationary phase condition to the remaining k integrand yields Fresnel-type integrals upon expansion about the stationary point. These integrals can then be solved analytically for times $t \gtrsim 1$. Keeping only the lowest order term in t we obtain the following expression for the dynamic contribution (see Appendix for details):

$$\mathcal{D}(v_p,t) \propto t^{-3/2} \cos\left(\frac{\pi}{4} + \nu_0 t\right) + O(t^{-5/2}), \tag{31}$$

where $\nu_0 = \sqrt{1 - v_p^2/3}$. A comparison with the full dielectric treatment of Sec. III A is shown in Fig. 4. The slight shift in the phase and the higher amplitudes are due to the approximation. For smaller velocities $v_p \ll 1$ the one-pole approximation shows rapidly increasing amplitudes while phase shift and periodicity remain unchanged; see Eq. (A4). In the case of an infinite magnetic field and if the ion is moving along the magnetic field lines an analogous treatment [Eqs. (A5)–(A8)] yields an expression similar to Eq. (31), which shows again a leading $O(t^{-3/2})$ time dependence and which compares to the full treatment for infinite magnetic field (Sec. III B) in a very resembling manner as displayed in Fig. 4 for the nonmagnetized case.

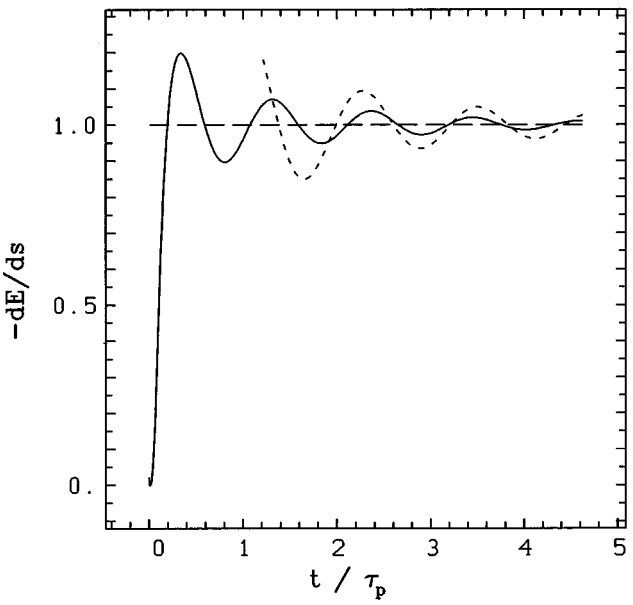

FIG. 4. Comparison of 1-pole approximation (short-dashed curve) with the full dielectric treatment (solid line) for $v_p = 1$ without magnetic field and $\mathcal{Z} = 0.94$. The corresponding asymptotic value from Table I is shown as long dashes.

IV. SHORT TIME BEHAVIOR

To get a better understanding of the processes forming the stopping power at very short time scales, we did a Taylor series expansion of the stopping power (11):

$$\frac{dE}{ds}(t) = \sum_n \frac{\partial^n}{\partial t^n} \frac{dE}{ds}\bigg|_{t=0} \frac{t^n}{n!}. \tag{32}$$

For practical reasons we started with a Fourier transformation of the Vlasov-Poisson equations (2) and (3) that enables us to analyze the potential ϕ^{tot} as well. The (linearized) total potential in $(\mathbf{k},t)$ space obeys the integral equation

$$\phi^{\mathrm{tot}}(\mathbf{k},t) = \underbrace{\frac{4\pi\mathcal{Z}}{k^2}\exp(-i\mathbf{k}\cdot\mathbf{v}_p t)}_{\phi^{\mathrm{ext}}} + \frac{i}{k^2}\int d^3v \left(\mathbf{k}\cdot\frac{\partial f_0}{\partial \mathbf{v}}\right) \underbrace{\int_0^t dt'\, \phi^{\mathrm{tot}}(\mathbf{k},t')\exp(i\mathbf{k}\cdot\mathbf{v}\,t'-t)}_{\mathcal{T}(t)} \tag{33}$$

with a differential equation for $\mathcal{T}(t)$:

$$\frac{\partial}{\partial t}\mathcal{T}(t) = -i\mathbf{k}\cdot\mathbf{v}\mathcal{T}(t) + \phi^{\mathrm{tot}}(t). \tag{34}$$

The expansion for the stopping power therefore reads

$$\frac{dE}{ds}(v_p,t) = -\frac{Z_p}{(2\pi)^3}\int d^3k \frac{\mathbf{k}\cdot\hat{\mathbf{v}}_p}{k^2}\int d^3v \cdot \mathbf{k}\frac{\partial f_0}{\partial \mathbf{v}}\sum_{n=0}^{\infty}\sum_{m=0}^{n}(i\mathbf{k}\cdot\mathbf{v}_p)^{n-m}\partial_t^m \mathcal{T}(t)\bigg|_{t=0}\frac{t^n}{n!}. \tag{35}$$

Within the following paragraphs we do not present any details of the calculations because they are quite straightforward despite their length and focus on the results only.

A. Linearized theory

With an appropriate choice of coordinates it is possible to integrate the **v** and **k** integrals up to $O(t^5)$. Due to symmetry arguments there is no contribution of any even order in t (stopping power must be real). This yields

$$\frac{dE}{ds}(v_p,t)=-\frac{\mathcal{Z}Z_p}{\pi}\left\{\frac{2}{27}v_p k_{\max}^3 t^3-\frac{1}{15}\left[\frac{v_p}{9}k_{\max}^3+\left(\frac{v_p^3}{25}+\frac{v_p}{5}\right)k_{\max}^5\right]t^5+O(t^7)\right\}, \tag{36}$$

where we have to use the same cutoff parameter $k_{\max}$ as before to keep the k integral finite. The same leading t^3 dependence is obtained in the case of an infinite magnetic field, where the perturbation f_1 depends only on $v_\parallel$.

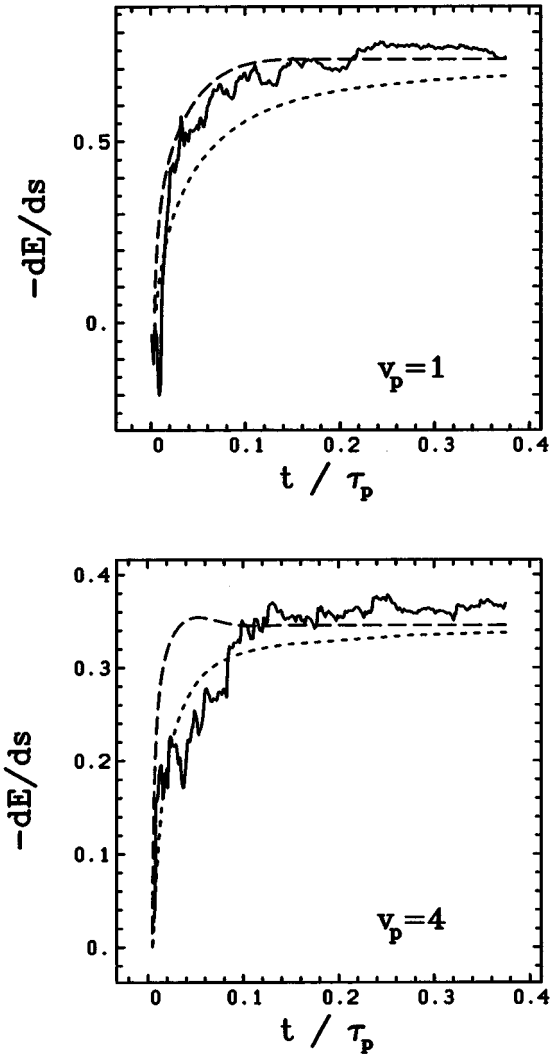

FIG. 5. Stopping power in units of $\mathcal{Z}Z_p k_B T/\lambda_D$ and for $\mathcal{Z}=0.03$ as a function of time from MD simulations (solid curve) and from the dielectric description before (long-dashed curve) and after (short-dashed) applying the average (38). The projectile velocity v_p is given in units of the thermal velocity $v_{\rm th}$.

B. Nonlinearized theory

As a further generalization we have applied the Taylor series expansion (32) also to the full Vlasov-Poisson equation without the usual linearization according to the value of coupling strength $\mathcal{Z}$. The analytic approach gets quite complex already at low orders in t and there is no chance for a handy recursion relation such as Eq. (34). Up to third order the stopping power is unchanged with respect to the previous result (36), in particular we also need a cutoff for the k integrals to stay finite:

$$\frac{dE}{ds}(v_p,t)=-\frac{\mathcal{Z}Z_p}{\pi}\frac{2}{27}v_p k_{\max}^3 t^3+O(t^5). \tag{37}$$

From symmetry considerations (stopping power has to be real) one can deduce that the next nonvanishing order will again be $O(t^5)$. This order will then show first contributions of the nonlinearity. Comparing Eqs. (36) and (37) we conclude therefore that a cutoff $k_{\max}$ must also be introduced in the nonlinear treatment.

V. MOLECULAR DYNAMICS SIMULATIONS

In order to extend the results of the dielectric treatment to stronger coupled plasmas ($\mathcal{Z}>1$) where nonlinear effects should become more important we have done molecular dynamics simulations for three different coupling strengths ($\mathcal{Z}=0.03$, 0.94, and 19.4) and four ion velocities ($v_p=1$, 4, 7, and 12 in units of $v_{\rm th}$).

A. Simulation technique

For the simulation the Newtonian equations of motion were integrated for $N=500$ electrons and the projectile with a given and constant charge. The plasma was treated classically with the interaction potential being the electrostatic Coulomb potential. The particles were constrained to a cubic simulation box with periodic boundary conditions and the long-range part of the Coulomb interaction treated by the Ewald sum [14]. To increase the performance of the simulation program a special cluster technique [15] has been implemented that allows a more accurate propagation of close particle encounters on smaller time scales while the overall system evolves on a larger time scale. Before the simulation, the plasma electrons (without projectile) were brought into equilibrium by thermalizing them to a desired temperature. Then, the ion was put into the simulation box. By using 200 statistically independent thermalized plasmas and different

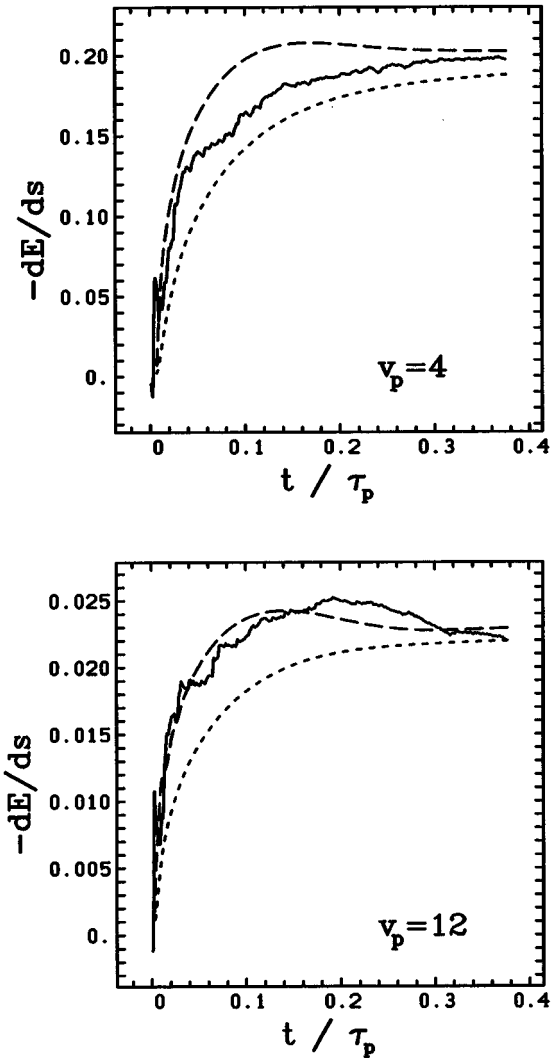

FIG. 6. Comparison of the stopping power from MD simulations and the dielectric treatment for $\mathcal{Z}=0.94$ (top) and $\mathcal{Z}=19.4$ (bottom). See Fig. 5 for the scaling and further details.

starting positions for the ion 1200 simulation runs were produced and averaged for each of the above 12 parameter sets. This huge data set was necessary to sufficiently improve statistics for a good time resolution.

To reduce the fluctuations in the simulation data due to close collisions an increasing average

$$\overline{\frac{dE}{ds}}(v_p,t)=\frac{1}{t}\int_0^t dt'\,\frac{dE}{ds}(v_p,t') \tag{38}$$

has been applied. All simulation data are displayed with this averaging method.

B. Comparison with dielectric theory

In order to compare the simulations with results of the dielectric theory we have to take into account the finite size L of the MD simulation box, which leads to a long wavelength cutoff. For the k integration in the dielectric treatment we used the lower boundary

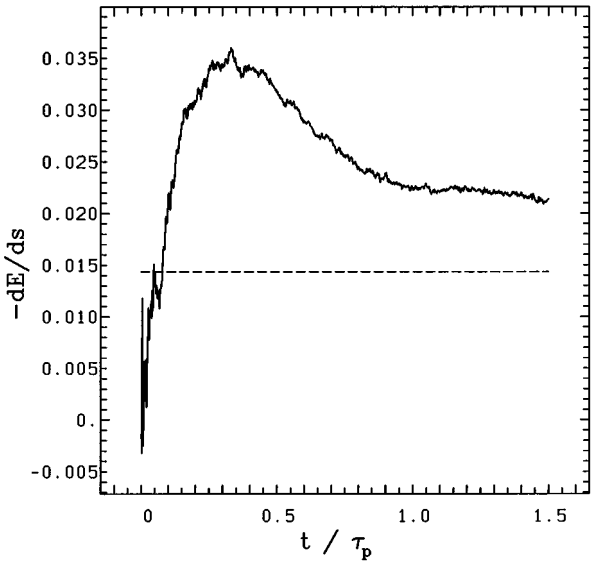

FIG. 7. Stopping power in units of $\mathcal{Z}Z_p k_B T/\lambda_D$ as a function of time from MD simulations for $\mathcal{Z}=19.4$ and $v_p=1$. Nonlinear contributions due to the strong coupling are responsible for a huge excess in stopping power and its slow decay to the stationary value (dashed line) obtained by MD simulations over 22 τ_p.

$$k_{\min}=\frac{2\pi}{L}. \tag{39}$$

Therefore the asymptotic values of the stopping power are slightly lower than those of Sec. III A (Table I). A comparison of results from the dielectric theory and MD simulations can be seen in Figs. 5 and 6 for $\mathcal{Z}=0.03$, 0.94, and 19.4 and different ion velocities v_p. The theoretical results are shown with and without the increasing average (38) to allow for a better assessment of its influence. Small oscillations are damped by this procedure. As the main feature a rapid onset of the stopping power within $\approx 0.25\tau_p$ is clearly visible in both approaches. About this typical time scale for the rise of the stopping power one can notice a tendency towards a somewhat shorter onset for increasing ion velocity at fixed coupling strength $\mathcal{Z}$ (Fig. 5) and a slower rise for increasing $\mathcal{Z}$ at the same velocity (Fig. 5, bottom and Fig. 6, top). For a sufficiently high projectile velocity the dielectric theory can still be used also for highly charged ions, i.e., large $\mathcal{Z}$ (see Fig. 6, bottom), in agreement with the condition for linearization $\mathcal{Z}/(1+v_p^3)\ll 1$ (5). As a contrast Fig. 7 shows the result of MD simulations for a strongly coupled plasma ($\mathcal{Z}=19.4$) and a slowly moving ion ($v_p=1$). Notice the strong excess in the stopping power near $0.5\tau_p$ that decays only slowly. It is due to nonlinear effects of the screening cloud that builds up behind the ion and persists because of its slow motion. Here the dielectric theory clearly has reached its limits.

VI. CONCLUSIONS

We present an extension to the well-known dielectric theory enabling us to describe the full time dependence of the stopping power for all ion velocities v_p without magnetic field and with an infinite magnetic field. In both cases we find a transient time of about a quarter plasma period τ_p for

a wide variety of ion-plasma coupling strengths $\mathcal{Z}$ and ion velocities v_p. This time constant should have a significant influence on the cooling properties of electron coolers as in ESR at the GSI in Darmstadt. The one-pole approximation yields a time evolution $O(t^{-3/2})$ close to the asymptotic regime. The Taylor series expansion of the stopping power for very short times reproduces the $O(t^3)$ behavior already mentioned by Avilov [9]. All these results do not depend significantly on the influence of an infinite magnetic field. Finally, we compare our analytic results in the field-free case with molecular dynamics computer simulations. The time constant $0.25\tau_p$ is also found in the MD simulations as long as the coupling does not get so large that the nonlinear effects of the interaction dominate.

ACKNOWLEDGMENTS

This work has been supported by the Bundesministerium für Bildung und Forschung (BMBF 06 ER 830 2), the Gesellschaft für Schwerionenforschung (GSI ER TOT), and the European Community (EU-HCM CHRX-CT94-0695 Ringnet).

APPENDIX: STOPPING POWER IN ONE-POLE APPROXIMATION

Applying the approximation of small k and v_p to Eq. (27) where $s_0(k)\approx -i\sqrt{1+3k^2}$ yields

$$\mathcal{D}(v_p,t)\approx -8\pi\int_0^{k_{\max}} dk k^3 \int_t^\infty d\tau \left(\frac{\sin(kv_p\tau)}{(kv_p\tau)^2}-\frac{\cos(kv_p\tau)}{kv_p\tau}\right)\frac{1}{2k^2}\sqrt{1+3k^2}\sin[\sqrt{1+3k^2}\tau]. \tag{A1}$$

To evaluate the k integral we expand about the point of stationary phase $k_0=v_p/(9-3v_p^2)^{-1/2}$. With $\nu(k)=\sqrt{1+3k^2}-kv_p$, $g(k)=k^{-1}\sqrt{1+3k^2}$ and $h(k)=\sqrt{1+3k^2}$, and $\nu_0=\nu(k_0)=\sqrt{1-v_p^{2/3}}$ we obtain

$$\mathcal{D}(v_p,t)\approx -2\pi^{3/2}\int_t^\infty d\tau\left\{-\frac{h_0}{v_p\sqrt{\nu_0''}}\tau^{-3/2}[\sin(\nu_0\tau)+\cos(\nu_0\tau)]-\left[\frac{g_0}{v_p^2\sqrt{\nu_0''}}-\frac{h_0''}{2v_p(\nu_0'')^{3/2}}\right]\tau^{-5/2}[\sin(\nu_0\tau)-\cos(\nu_0\tau)]\right.$$
$$\left.-\frac{g_0''}{2v_p^2(\nu_0'')^{3/2}}\tau^{-7/2}[\sin(\nu_0\tau)+\cos(\nu_0\tau)]\right\} \tag{A2}$$

for the dynamic contribution. The remaining τ integral can be reduced to Fresnel-type integrals [16]

$$\int_0^z du\cos\left(\frac{\pi}{2}u^2\right)=C(z),\quad \int_0^z du\sin\left(\frac{\pi}{2}u^2\right)=S(z). \tag{A3}$$

Expanding the $C(z),S(z)$ functions for large arguments (i.e., $t\to\infty$) allows for analytic expressions after collecting all terms up to lowest order in t:

$$\mathcal{D}(v_p,t)\approx\frac{(2\pi)^{3/2}}{v_p}\left(\frac{3^5}{(3-v_p^2)^7}\right)^{1/4}t^{-3/2}\cos\left[\nu_0 t+\frac{\pi}{4}\right]. \tag{A4}$$

For an infinite magnetic field, where the ion is moving parallel to the field lines, we have to use a slightly different dielectric function (19), which in turn gives raise to a slightly different dynamic contribution (30). Applying the same approximations as in the field-free case ($k\ll 1$, $v_p\ll 1$ and $t\gg 1$) yields

$$\mathcal{D}_\infty(v_p,t)\approx 2\pi\int_0^{k\max} dk k\sqrt{1+3k^2}\int_0^1 d\mu \times\mu\left(\frac{\sin(\nu_-\mu t)}{\nu_-}+\frac{\sin(\nu_+\mu t)}{\nu_+}\right), \tag{A5}$$

with $\nu_\pm(k)=\sqrt{1+3k^2}\pm kv_p$.

Hence, using the stationary phase argument again, we evaluate the μ integral to obtain

$$\mathcal{D}_\infty(v_p,t)\approx 2\pi\int_0^{k\max} dk\frac{k\sqrt{1+3k^2}}{\nu_-^2}\left(\frac{\sin(\nu_- t)}{\nu_- t^2}-\frac{\cos(\nu_- t)}{t}\right). \tag{A6}$$

Introducing two new k-dependent functions

$$g(k)=\frac{k\sqrt{1+3k^2}}{\nu_-^2 t}\quad\text{and}\quad h(k)=\frac{k\sqrt{1+3k^2}}{\nu_-^3 t^2} \tag{A7}$$

enables us to expand the integral analogously to Eq. (A2). This yields

$$\mathcal{D}_\infty(v_p,t)\approx -(2\pi)^{3/2}v_p\left(\frac{3^5}{(3-v_p^2)^{11}}\right)^{1/4}t^{-3/2}\cos\left[\nu_0 t+\frac{\pi}{4}\right] \tag{A8}$$

for the infinite magnetic field.

[1] E. Nardi and Z. Zinamon, Phys. Rev. Lett. **49**, 1251 (1982).
[2] T. Peter and J. Meyer-ter-Vehn, Phys. Rev. A **43**, 1998 (1991).
[3] A. H. Sørensen and E. Bonderup, Nucl. Instrum. Methods **215**, 27 (1983).
[4] G. Zwicknagel, C. Seele, M. Miller, C. Toepffer, and P.-G. Reinhard, Laser Part. Beams **13**, 311 (1995).
[5] G. Zwicknagel, P.-G. Reinhard, C. Seele, and C. Toepffer, Fusion Eng. Des. **32-33**, 523 (1996).
[6] J. D'Avanzo and I. Hofmann, GSI Report 1994, GSI-95-06, 45 (1995).
[7] O. Boine-Frankenheim, Phys. Plasmas **3**, 1585 (1996).
[8] O. Boine-Frankenheim and J. D.'Avanzo, Phys. Plasmas **3**, 792 (1996).
[9] V. V. Avilov, in CERN Report No. CERN 94-03, 227 (1994).
[10] G. Zwicknagel and C. Deutsch, Phys. Rev. E **56**, 970 (1997).
[11] B. D. Fried and S. D. Conte, *The Plasma Dispersion Function* (Academic Press, New York, 1961).
[12] L. D. Landau and E. M. Lifshitz, *Physical Kinetics*, Course of Theoretical Physics Vol. 10 (Pergamon Press, New York, 1981) Chap. 3.
[13] S. Ichimaru, *Basic Principles of Plasma Physics* (Benjamin, Reading, MA 1973), Sec. 10.3.
[14] B. R. A. Nijboer and F. W. De Wette, Physica (Amsterdam) **23**, 309 (1957).
[15] G. Zwicknagel, Ph.D. thesis, Universität Erlangen, 1994.
[16] *Handbook of Mathematical Functions*, edited by M. Abramowitz and I. A. Stegun (Dover, New York, 1972).